

# Effect of prism material on design of surface plasmon resonance sensor by admittance loci method

Kaushik BRAHMACHARI, Mina RAY (✉)

Department of Applied Optics and Photonics, University of Calcutta, Kolkata 700 009, India

© Higher Education Press and Springer-Verlag Berlin Heidelberg 2013

**Abstract** A theoretical study on the design of surface plasmon resonance (SPR) based sensor by admittance loci method has been reported in this paper with the main emphasis being given to the effect of the prism material in a conventional Kretschmann structure in attenuated total internal reflection (ATIR) mode. Several sensing media such as water, acetone, methanol etc have been investigated using different types of prism materials to study their effect on SPR sensing and validated by corresponding admittance loci plots as well as respective SPR curves. The performance of the sensor based on choice of the prism material has been discussed with the help of sensitivity plots giving due to the importance of dynamic range of the designed sensor. Simulations have been carried out in MATLAB 7.1 environment.

**Keywords** admittance loci method, surface plasmon resonance (SPR), thin film, sensors, multilayer structure

## 1 Introduction

Surface plasmon resonance (SPR) phenomenon is the surface charge density oscillation at a metal-dielectric interface due to p-polarized incident light. The basic prism based configurations of SPR device were proposed before for observing SPR [1,2]. It has been widely applied for sensing various samples. The first application of SPR phenomenon as a sensing tool was observed in gas detection and biosensing [3]. SPR was also used for sensing of different chemical and biological samples [4,5]. Experimental observation of SPR using various geometrical configurations of metal-dielectric interface has been reported earlier [6–8]. Admittance loci method has been used in thin film modeling [9] and design of SPR based devices [10–13]. Some studies related to sensing

application of admittance loci method have been reported [14–16]. Chen et al. has worked on localized SPR sensor [17]. An improved sensitivity using high refractive-index ceramic substrate for surface plasmon sensing has also been reported [18]. Moreover, there are lots of different approaches to define the sensitivity parameter depending upon the method of interrogation as well as the application concerned.

This paper first describes the well-established admittance loci method and then its subsequent use to study substrate (glass prism) dependency of a sensor comprising of a multilayer structure based on SPR phenomenon. Sensitivity issues regarding the use of different glass materials are also discussed with a somewhat different approach to qualitatively visualize this dependency.

## 2 Mathematical background

Based on the approach of Macleod [9], we present a multilayer structure consisting of incident medium (glass prism), metal film and sample as shown in Fig. 1. The interfaces among the film, the incident medium and the sample are denoted by the symbols  $a$  and  $b$  respectively.  $z$  is the normal to film boundaries.  $n_p$ ,  $n_m$  and  $n_{\text{sample}}$  are the refractive indices of incident medium (glass prism), metal film and sample respectively. Admittance of a multilayer structure starts from sample and ends at front surface of the multilayer structure.

For absorbing metal layer, the phase is given by

$$\delta_m = \left( \frac{2\pi}{\lambda} \right) d_m (n_m^2 - k_m^2 - n_p^2 \sin^2 \theta_i - 2in_m k_m)^{1/2}, \quad (1)$$

where  $n_m$ ,  $k_m$  and  $d_m$  are the real and imaginary part of the complex refractive index and thickness of the absorbing metal layer respectively and  $\lambda$  is the wavelength of incident light.

The tangential components of electric ( $E$ ) and magnetic ( $H$ ) fields at the interface  $a$  and  $b$  are related by a

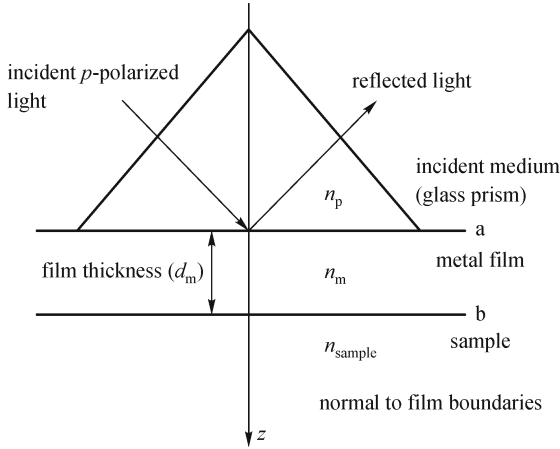


**Fig. 1** Multilayer structure consisting of incident medium (glass prism), metal film and sample

characteristics matrix as given by

$$\begin{bmatrix} E_a \\ H_a \end{bmatrix} = \begin{bmatrix} \cos\delta_m & (i\sin\delta_m)/\eta_m \\ i\eta_m\sin\delta_m & \cos\delta_m \end{bmatrix} \begin{bmatrix} E_b \\ H_b \end{bmatrix}. \quad (2)$$

So we can write the admittance of the multilayer structure as

$$Y = \frac{H_a}{E_a} = \frac{C}{B} = \frac{\eta_{\text{sample}}\cos\delta_m + i\eta_m\sin\delta_m}{\cos\delta_m + i(\eta_{\text{sample}}/\eta_m)\sin\delta_m}, \quad (3)$$

where  $B$  and  $C$  are the normalized electric and magnetic fields at the interface  $a$ , using which the properties of the thin film can be evaluated.

The reflectance of a multilayer structure ( $R$ ) is given by

$$R = \left( \frac{\eta_p - Y}{\eta_p + Y} \right) \left( \frac{\eta_p - Y}{\eta_p + Y} \right)^*, \quad (4)$$

where  $\eta_p$ ,  $\eta_m$ ,  $\eta_{\text{sample}}$  are the admittances of incident medium (glass prism), metal film and sample respectively and ‘\*’ denotes the complex conjugate.

A way to describe the performance of the SPR based structure is to plot isorefectance contours in the admittance diagram. Isorefectance contours are the circles with centers on real axis, centers and radii being given by  $(\eta_p(1+R)/(1-R), 0)$  and  $2\eta_p(R)^{1/2}/(1-R)$ , where  $\eta_p$  is the admittance of the incident medium (glass prism) and  $R$  is the reflectance.

At oblique incidence, the modified optical admittances are given by

For dielectric samples:

$$\eta_{\text{sample}}^s = \frac{y_{\text{sample}}\cos\theta_{\text{sample}}}{\cos\theta_i}, \quad (5)$$

$$\eta_{\text{sample}}^p = \frac{y_{\text{sample}}\cos\theta_i}{\cos\theta_{\text{sample}}}, \quad (6)$$

where  $y_{\text{sample}} = n_{\text{sample}}y_f$  is the optical admittance and  $y_f$  is the admittance of free space and its value is unity in Gaussian units.

For absorbing metal film:

$$\eta_m^s = \frac{(n_m^2 - k_m^2 - n_p^2 \sin^2\theta_i - 2in_mk_m)^{1/2}}{\cos\theta_i}, \quad (7)$$

$$\eta_m^p = \frac{(n_m - ik_m)^2}{\eta_m^s}, \quad (8)$$

where the superscripts  $s$  and  $p$  denote polarization states of the incident light,  $\theta_i$  is the angle of incidence and  $\theta_{\text{sample}}$  is the angle corresponding to sample layer.

As proposed by Homola et al. [5], the propagation constant of a surface plasmon wave (SPW) at the interface between metal and dielectric sample can be written as

$$k_{\text{SPW}} = k_0 \sqrt{\frac{\epsilon_m n_{\text{sample}}^2}{\epsilon_m + n_{\text{sample}}^2}}. \quad (9)$$

The real part of propagation constant of a SPW wave is given by

$$\text{Re}(k_{\text{SPW}}) \cong k_0 \sqrt{\frac{\epsilon_{\text{mr}} n_{\text{sample}}^2}{\epsilon_{\text{mr}} + n_{\text{sample}}^2}}. \quad (10)$$

The coupling condition is given by

$$k_0 n_p \sin\theta_{\text{SPR}} = k_0 \sqrt{\frac{\epsilon_{\text{mr}} n_{\text{sample}}^2}{\epsilon_{\text{mr}} + n_{\text{sample}}^2}}, \quad (11)$$

where  $\epsilon_m$  is the dielectric constant of the metal (absorbing in nature),  $\epsilon_{\text{mr}}$  is the real part of dielectric constant of the mentioned metal,  $k_0$  is the free space wave number and  $\theta_{\text{SPR}}$  is the SPR angle.

The sensitivity ( $S$ ) of an SPR sensor in angular interrogation mode is defined as the ratio of the shift in SPR angle ( $d\theta_{\text{SPR}}$ ) to the change in refractive index of the sample ( $dn_{\text{sample}}$ ) and is given by Ref. [5].

$$S = \frac{d\theta_{\text{SPR}}}{dn_{\text{sample}}} = \frac{\left( \frac{\epsilon_{\text{mr}}}{\epsilon_{\text{mr}} + n_{\text{sample}}^2} \right)^{3/2}}{\sqrt{n_p^2 - \frac{\epsilon_{\text{mr}} n_{\text{sample}}^2}{\epsilon_{\text{mr}} + n_{\text{sample}}^2}}}. \quad (12)$$

### 3 Results and discussion

In this work, the admittance loci method has been used to design and analyze the multilayer structure concerned with SPR based sensing with the emphasis on the role of the prism material. To investigate the effect of glass material in such structures, different glass prism materials have been

used in a basic three-layer Kretschmann structure consisting of glass prism|gold film ( $\sim 50$  nm)|sample. The MATLAB simulations have been carried out with three samples, namely water, acetone, methanol and few more samples where water was taken as a reference sample. Figure 2(a) shows the admittance loci plot with isoreflectance contours for BK7 glass prism as an incident medium and water as sample. Simulated admittance loci plots demonstrate that the starting admittance for the gold film is on the imaginary axis. It also shows near zero reflectance at a particular angle of incidence and metal thickness. In this case, the locus point moves from the value of  $0.832i$  (gold film thickness =  $0$  nm) on the imaginary axis and ends at the value of  $1.492$  (gold film thickness =  $50$  nm) on the real axis (which is quite close to  $n_{pBK7} = 1.51508$ ) for an angle of incidence  $73.96^\circ$ . Similarly as shown in Fig. 2(b), as an incident medium is SF10 glass prism, the locus point moves from value of  $1.536i$  on imaginary axis and ends at value of  $1.643$  (quite close to  $n_{pSF10} = 1.72312$ ) on real axis for an angle of incidence  $58.18^\circ$ . If we could have made this locus to

intercept the real axis of the admittance diagram at the refractive index of the incident medium depending upon the glass prism type we are using (e.g., BK7, SF10), the excitation of the surface plasmon would have been achieved with maximum efficiency. Figure 2(c) shows admittance loci plot of the SPR based structure for BK7 prism and water as a sample for three different gold metal film thicknesses of  $45$ ,  $50$  and  $55$  nm, respectively. It can be seen from the plot that starting imaginary admittance values are  $0.8528i$ ,  $0.832i$ ,  $0.8102i$  and end real admittance values are  $1.571$ ,  $1.492$  (close to the value of refractive index of BK7 prism, which is  $1.51508$ ),  $1.172$  for  $45$ ,  $50$  and  $55$  nm gold film thicknesses at incident angles of  $73.69^\circ$ ,  $73.96^\circ$ ,  $74.25^\circ$ , respectively. From these results, it can be concluded that  $50$  nm is the ideal thickness to achieve efficient plasmonic excitation.

Many more similar simulated results using admittance loci method for three glass prism materials, like, BK7, SF5 and SF11, with water as sample have been shown in Figs. 3(a). Same procedures have been repeated with methanol and acetone samples respectively as shown in

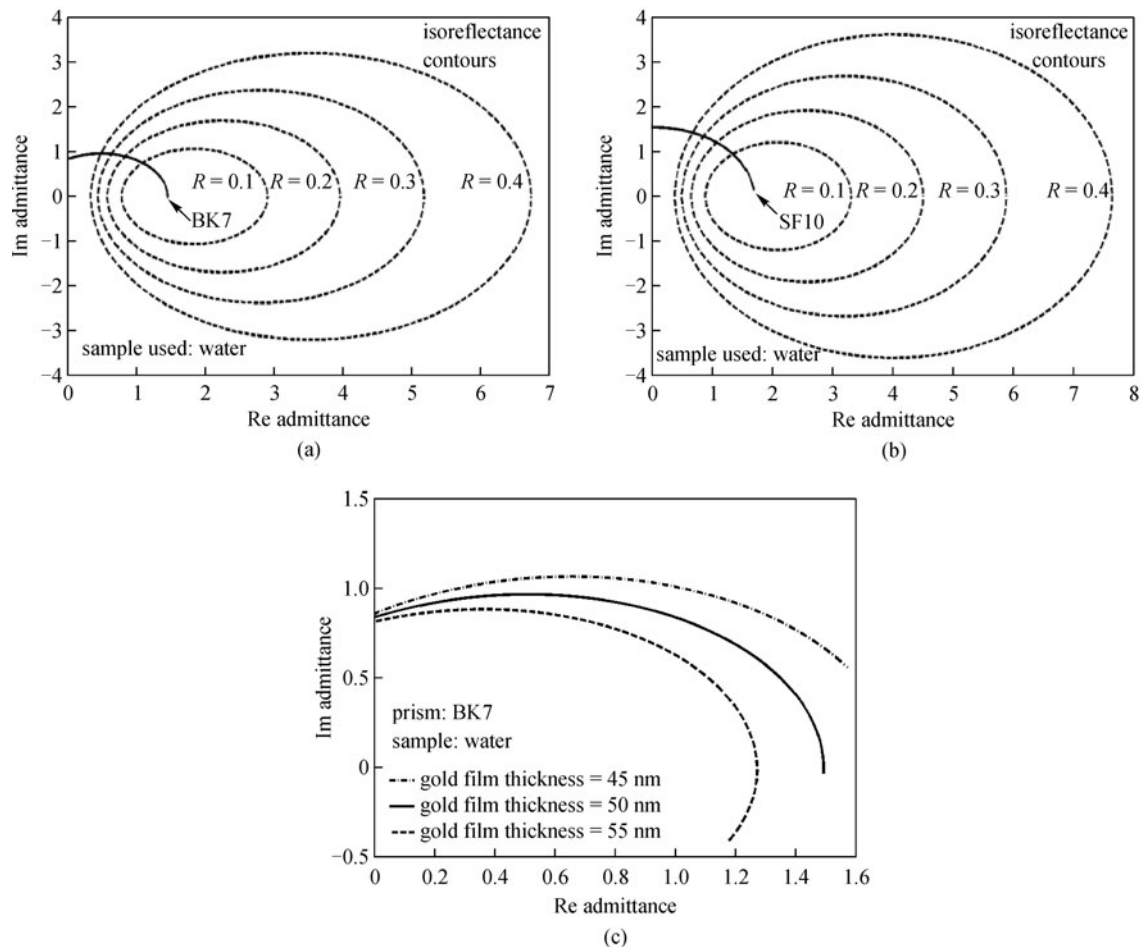


**Fig. 2** Admittance loci plot of 3-layer structure with isoreflectance contours for glass prisms (a) BK7; (b) SF10; and (c) BK7 (without isoreflectance contours) for gold film thicknesses of  $45$ ,  $50$  and  $55$  nm, respectively

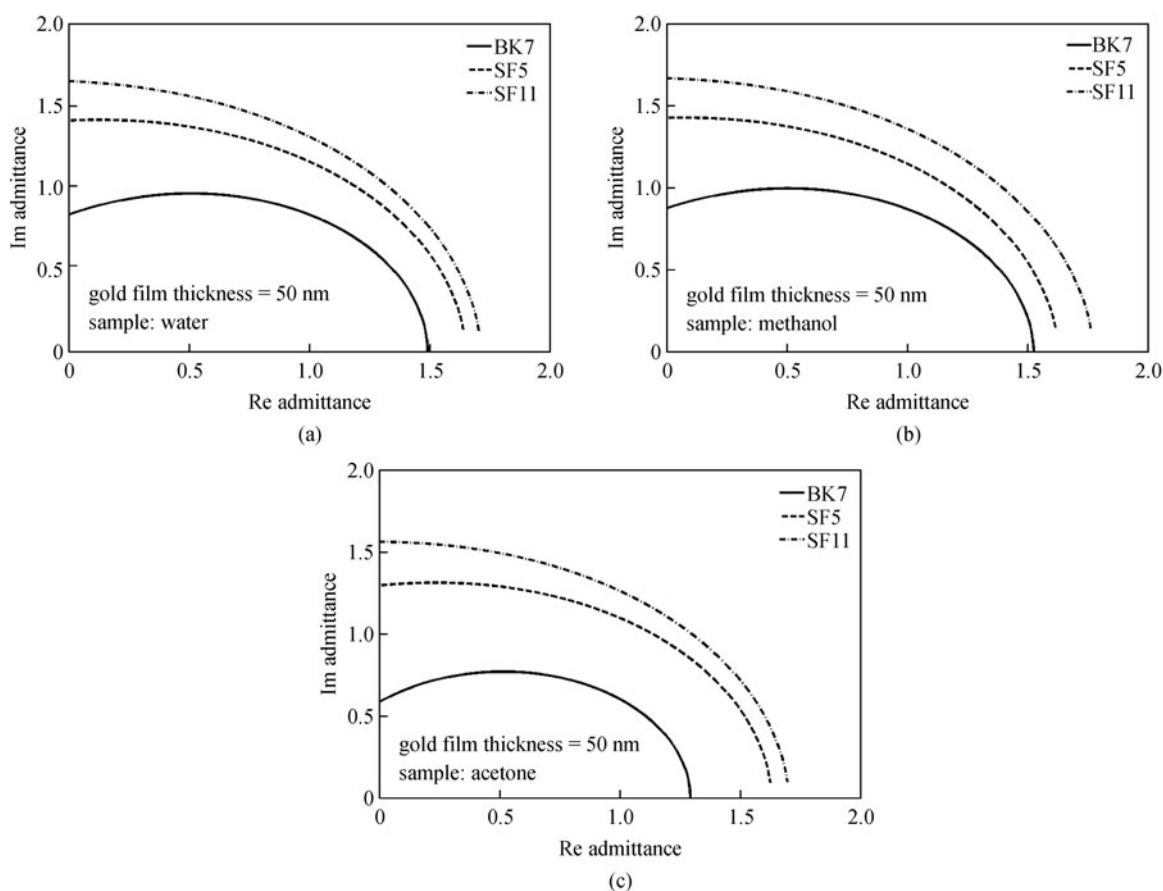


**Fig. 3** Admittance loci plot of 3-layer structure for BK7, SF5 and SF11 glass prisms with (a) water; (b) methanol and (c) acetone as samples

Figs. 3(b) and 3(c). The values of starting and ending admittance and angle of incidence using gold metal film with fixed thickness of 50 nm, for water, acetone and methanol as samples are presented in Table 1, where the working wavelength is 633 nm. Table 2 shows the values of refractive indices (real part and imaginary part) of different materials used in the SPR based structure.

In all these cases, we have optimized the angle of incidence and fixed the gold film thickness at 50 nm for each prism material, so as to ensure that the respective loci end with real admittance close to the value of refractive index of the prism as far as possible, which in turn ensures the most efficient excitation of surface plasmon.

Resonance curves are based on the simulation using conventional characteristics transfer matrix formalism based on Fresnel reflection coefficient for multilayer stack. Theoretical values of SPR angle, at which the reflectance is the minimum, can be obtained from respective resonance curves. Simulations have been done in MATLAB 7.1 environment. Figure 4(a) depicts the resonance curves for three prism materials BK7, SF5 and SF11 with samples, such as water, acetone and methanol. Figure 4(b) shows the resonance curves for all the prism

materials under consideration with water as the reference sample. Gold film thickness is kept at 50 nm throughout the simulations.

The sensitivity as given by Eq. (12) can be theoretically evaluated using the simulated plots. Moreover, full width half maximum (FWHM) is also an important factor to be considered for the actual design of a sensor. Based on the data denoted in Table 3, we obtained the changes of FWHM, SPR angle, angular shift for water-acetone and water-methanol combinations with corresponding glass prism refractive index as indicated in Figs. 5(a)–5(c). Water is taken as a reference sample in both cases. The sensor parameters, namely FWHM, SPR angle and angular shift, are found to decrease with increase in glass prism refractive index values. Table 4 shows the SPR angle, angular shift and sensitivity data of the sensor. Figures 5(d) and 5(e) show the plot of SPR angle vs. sample refractive index and the variation of sensitivity with sample refractive index for three glass prism materials, namely BK7, SF5, SF11. Here for these calculations, the sample refractive index is varied from 1.33 to 1.38. From both the plots, it can be concluded that SPR angle and sensitivity both increase with increase in sample refractive index values.

**Table 1** Values of admittance and angle of incidence for different samples and prism materials

glass prism	samples								
	water			acetone			methanol		
	$\eta_{si}$	$\eta_{er}$	$\theta_i$	$\eta_{si}$	$\eta_{er}$	$\theta_i$	$\eta_{si}$	$\eta_{er}$	$\theta_i$
BK7	0.832i	1.492, -0.03742i	73.96	0.5855i	1.249, -0.2538i	78.91	0.8749i	1.525, -0.008716i	73.09
BAK1	1.092i	1.528, 0.09669i	68.38	0.9277i	1.492, 0.002443i	71.85	1.123i	1.544, 0.1094i	67.72
BAF10	1.407i	1.663, 0.1348i	61.32	1.296i	1.67, 0.09242i	63.81	1.425i	1.606, 0.1358i	60.87
SF5	1.409i	1.64, 0.1331i	61.25	1.297i	1.624, 0.09427i	63.75	1.429i	1.617, 0.137i	60.78
SF10	1.536i	1.643, 0.1264i	58.18	1.442i	1.662, 0.1012i	60.37	1.555i	1.64, 0.1303i	57.75
SF11	1.649i	1.705, 0.1243i	55.44	1.563i	1.695, 0.09822i	57.43	1.67i	1.762, 0.1402i	55.02

Notes: 1) Gold film thickness is 50 nm for all the samples

2)  $\eta_{si}$  and  $\eta_{er}$  represent the starting imaginary admittance values and ending admittance values respectively.  $\theta_i$  is the corresponding angle of incidence in degrees

**Table 2** Refractive indices of different materials

materials	refractive index
BK7 glass	1.51508
BAK1 glass	1.5704
BAF10 glass	1.66707
SF5 glass	1.66846
SF10 glass	1.72312
SF11 glass	1.77858
gold (Au)	0.16172 + 3.21182i
water	1.33168
methanol	1.32634
acetone	1.35781

Also, the values of SPR angle and sensitivity are higher for lower index glass (BK7) and lower for higher index glass (SF11). The dynamic range is an important feature of an SPR sensor. The dynamic range is defined as the range of dielectric samples, which can be sensed and governed by plasmon resonance condition. The maximum value of the refractive index of the sample that can be sensed for a particular sensor structure can be obtained using Eq. (11), for which  $\sin\theta_{SPR}$  is just less than 1. For a BK7 glass prism ( $n_{pBK7} = 1.51508$ ), the sample refractive index for which  $\theta_{SPR} = 90^\circ$  was calculated to be  $(n_{sample})_{max} = 1.3700$ , beyond which it is not possible to detect the sample. So, with BK7 glass prism, all the dielectric samples with refractive indices less than 1.3700 are detectable. Similarly, for SF5 and SF11 glass prisms, these limits are 1.4802 and 1.5555 respectively, which shows that the dynamic range of the sensor is reduced by using the prism with lower refractive index (BK7) compared to higher

refractive index (SF11). These results are in good agreement with those shown in Ref. [19]. So, one should choose the prism material depending on the application concerned with a compromise between the sensitivity and the dynamic range. For sensing broad range of samples, it is not preferable to reduce the refractive index of the prism. However, if the ranges of samples are fixed and known, we can use low index prism.

## 4 Conclusions

We have reported the glass prism material dependency of a SPR sensor with a multilayer structure using admittance loci method. In this work, we have used different glass materials for prisms in order to see the effect of these glasses on admittance loci plots of the multilayer structure considered and also on SPR sensing, keeping the sample layer same. We have also used different samples like water, acetone, methanol and few more samples to study various parameters of SPR sensing, namely FWHM, SPR angle, angular shift, sensitivity, etc. The parameters are found to be greatly influenced by index of the glass prisms used. It is also evident from the simulation curves that the glass of higher refractive index material gives very sharp resonance curves in comparison to the lower refractive index glasses, which may provide greater measurement precision in sensing applications. However, values of FWHM, SPR angle, angular shift and sensitivity are larger for lower index glass material compared to higher one at the visible wavelength concerned. Our sensitivity plot suggests to select low index glass material instead of higher index glass while operating the sensor at 633 nm wavelength due to its higher sensitivity. But using low refractive index prisms reduces the dynamic range of the sensor and also

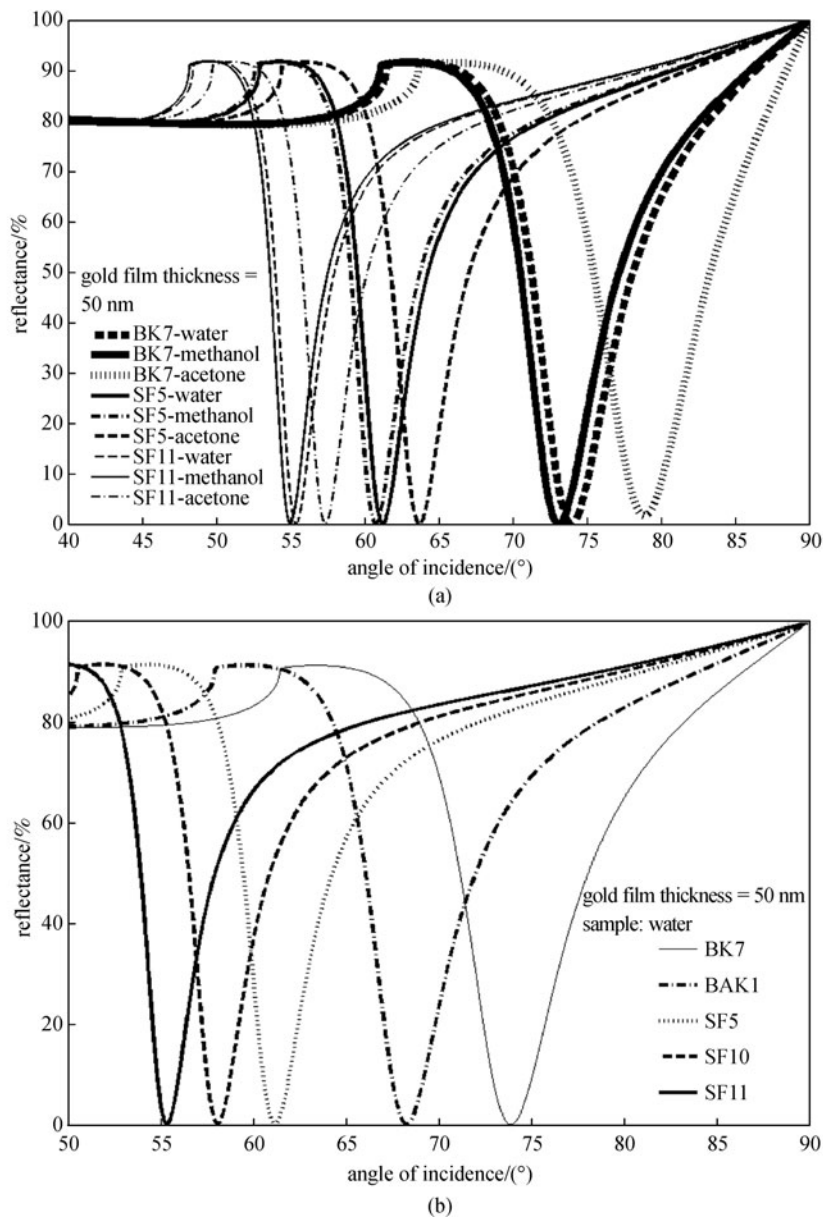


**Fig. 4** SPR curves for (a) BK7, SF5 and SF11, each with three samples indicated in the legend and (b) all prism materials with water as the reference sample

**Table 3** Values of SPR angle, angular shift and FWHM for different glass materials for three samples

glass prism	samples								
	water			acetone			methanol		
	SPR angle/(°)	angular shift/(°) w.r.t water	FWHM/(°)	SPR angle/(°)	angular shift/(°) w.r.t water	FWHM/(°)	SPR angle/(°)	angular shift/(°) w.r.t water	FWHM/(°)
BK7	73.99	0	6.91	78.91	4.92	7.92	73.11	0.88	6.72
BAK1	68.34	0	5.95	71.78	3.44	6.71	67.69	0.65	5.8
BAF10	61.32	0	4.83	63.81	2.49	5.33	60.84	0.48	4.72
SF5	61.24	0	4.83	63.72	2.48	5.34	60.76	0.48	4.73
SF10	58.14	0	4.37	60.34	2.2	4.81	57.71	0.43	4.32
SF11	55.42	0	4.02	57.39	1.97	4.43	55.02	0.4	3.94

Note: Gold film thickness is 50 nm for all samples used here

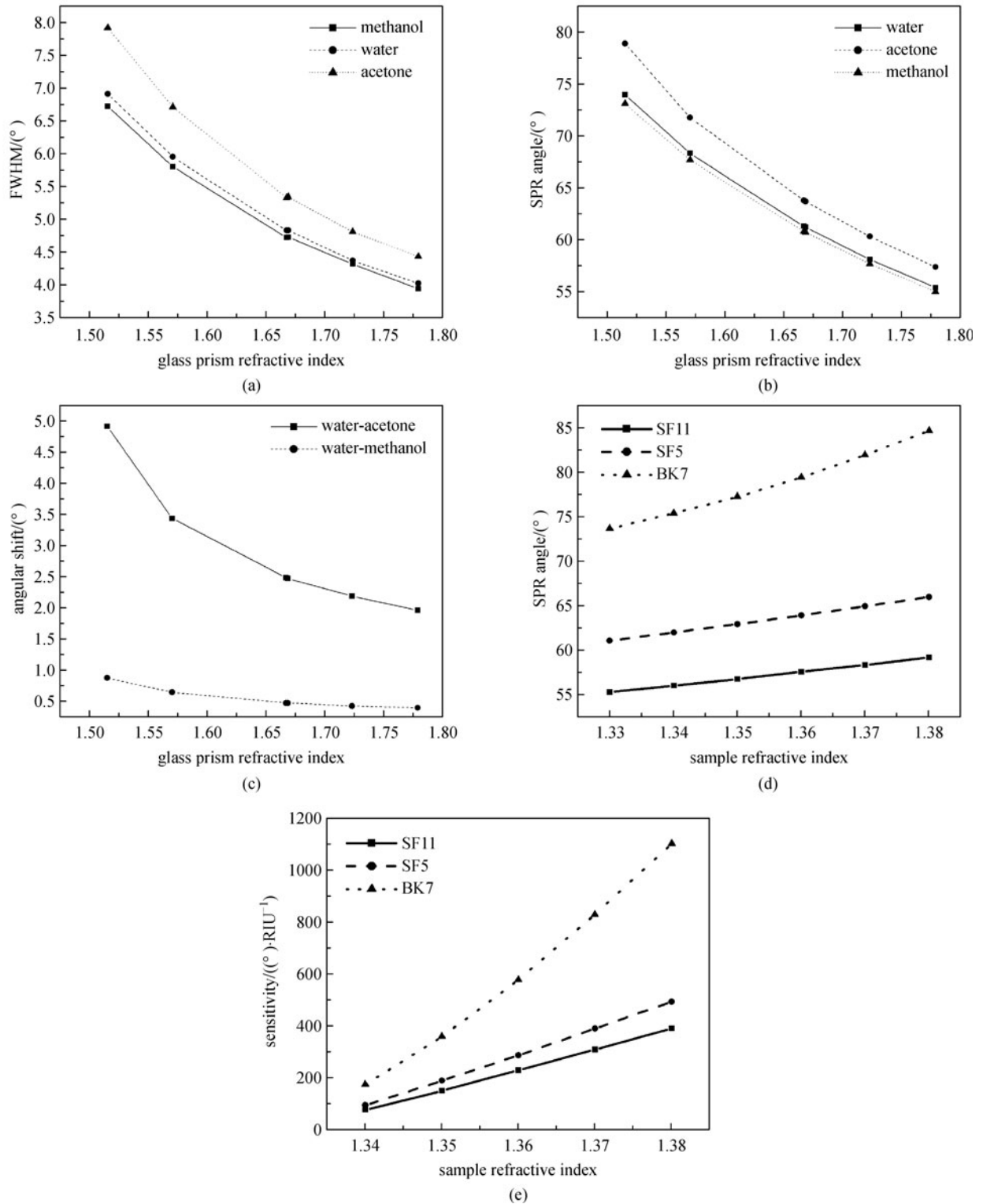


**Fig. 5** Plot of (a) FWHM; (b) SPR angle; (c) angular shift vs. glass prism refractive indices for three samples and (d) SPR angle; (e) sensitivity vs. sample refractive index for three prism materials

**Table 4** Values of SPR angle, angular shift and sensitivity for three glass materials for different samples

sample refractive index	glass prisms								
	BK7			SF5			SF11		
	SPR angle/(°)	angular shift/(°)	sensitivity/(°·RIU <sup>-1</sup> )	SPR angle/(°)	angular shift/(°)	sensitivity/(°·RIU <sup>-1</sup> )	SPR angle/(°)	angular shift/(°)	sensitivity/(°·RIU <sup>-1</sup> )
1.33	73.68	0	0	61.09	0	0	55.3	0	0
1.34	75.4	1.72	172	62.01	0.92	92	56.04	0.74	74
1.35	77.25	3.57	357	62.96	1.87	187	56.78	1.48	148
1.36	79.43	5.75	575	63.94	2.85	285	57.57	2.27	227
1.37	81.95	8.27	827	64.97	3.88	388	58.37	3.07	307
1.38	84.68	11	1100	66.01	4.92	492	59.19	3.89	389

Note: Gold film thickness is 50 nm for all samples used here

increases the FWHM of the SPR curve. So, one can conclude that low index prism material is preferable for the applications, where higher sensitivity is required and range of sample refractive indices is narrow. The choice of prism material must be in accordance with the application concerned keeping in mind the optimized trade-off between the sensitivity and dynamic range requirements.

**Acknowledgements** This work was supported by Centre for Research in Nanoscience and Nanotechnology (CRNN), University of Calcutta, Kolkata, India. K. Brahmachari also wants to thank Technical Education Quality Improvement Program (TEQIP PhaseII), University of Calcutta for providing Senior Research Assistantship to carry out this work.

## References

- Otto A. Excitation of nonradiative surface plasma waves in silver by the method of frustrated total reflection. *Zeitschrift fur Physik*, 1968, 216(4): 398–410
- Kretschmann E, Raether H. Radiative decay of non-radiative surface plasmons excited by light. *Zeitschrift fur Naturforschung. Teil B. Anorganische Chemie, Organische Chemie, Biochemie, Biophysik, Biologie*, 1968, 23A: 2135–2136
- Liedberg B, Nylander C, Lunström I. Surface plasmon resonance for gas detection and biosensing. *Sensors and Actuators*, 1983, 4: 299–304
- Homola J, Yee S S, Gauglitz G. Surface plasmon resonance sensor: review. *Sensors and Actuators B, Chemical*, 1994, 54(1–2): 3–15
- Homola J, Koudela I, Yee S S. Surface plasmon resonance sensors based on diffraction gratings and prism couplers: sensitivity comparison. *Sensors and Actuators B, Chemical*, 1999, 54(1–2): 16–24
- Brahmachari K, Ghosh S, Ray M. Experimental observation of surface plasmon resonance using various geometrical configurations of metal-dielectric interface. In: *Proceedings of the International symposium on Advances in Nanomaterials*, CSIR-Central Glass & Ceramic Research Institute, Kolkata, India, 2010
- Ghosh S, Brahmachari K, Ray M. Experimental investigation of surface plasmon resonance using a chemically deposited silver film on a tapered cylindrical glass rod. In: *Proceedings of the International Conference on Specialty Glass & Optical Fiber: Materials, Technology & Devices*, CSIR-Central Glass & Ceramic Research Institute, Kolkata, India, 2011
- Ghosh S, Brahmachari K, Ray M. Experimental investigation of surface plasmon resonance using tapered cylindrical light guides with metal-dielectric interface. *Journal of Sensor Technology*, 2012, 2(1): 48–54
- Macleod A H. *Thin-Film Optical Filters*. 4th ed. New York: CRC Press, 2010
- Lin W C, Chen P K, Su C M, Lee K C, Yang C C. Bio-plasmonics: nano/micro structure of surface plasmon resonance devices for biomedicine. *Optical and Quantum Electronics*, 2005, 37(13–15): 1423–1437
- Lin W C, Chen P K, Su C M, Hsiao C T, Lee S S, Lin S, Shi J X, Lee K C. Admittance loci design method for multilayer surface plasmon resonance devices. *Sensors and Actuators B, Chemical*, 2006, 117(1): 219–229
- Lin W C, Chen P K, Hsiao N C, Lin S, Lee K C. Design and fabrication of an alternating dielectric multi-layer device for surface plasmon resonance sensor. *Sensors and Actuators B, Chemical*, 2006, 113(1): 169–176
- Jen Y J, Lakhtakia A, Yu C W, Chan T Y. Multilayered structures for p- and s-polarized long-range surface-plasmon-polariton propagation. *Journal of the Optical Society of America A, Optics, Image Science, and Vision*, 2009, 26(12): 2600–2606
- Brahmachari K, Ghosh S, Ray M. Application of admittance loci method in surface plasmon resonance technology for sensing of different chemical and biological samples. In: *Proceedings of the International Conference on Specialty Glass & Optical Fiber: Materials, Technology & Devices*, CSIR-Central Glass & Ceramic Research Institute, Kolkata, India, 2011
- Brahmachari K, Ghosh S, Ray M. Substrate dependence of surface plasmon resonance sensor with a multilayer structure using admittance loci method. In: *Proceedings of 2nd International Conference on Trends in Optics and Photonics*, Kolkata, India, 2011, 402–407
- Brahmachari K, Ghosh S, Ray M. Surface plasmon resonance based sensing of different chemical and biological samples using admittance loci method. *Photonic Sensors*, 2012, doi:10.1007/s13320-012-0062-7

17. Chen Y, Ming H. Review of surface plasmon resonance and localized surface plasmon resonance sensor. *Photonic Sensors*, 2012, 2(1): 37–49
18. Micheletto R, Hamamoto K, Fuji T, Kawakami Y. Tenfold improved sensitivity using high refractive-index substrates for surface plasmon sensing. *Applied Physics Letters*, 2008, 93(17): 1741041–1741043
19. Gupta G, Kondoh J. Tuning and sensitivity enhancement of surface plasmon resonance sensor. *Sensors and Actuators B, Chemical*, 2007, 122(2): 381–388